The CO poisoning effect in PEMFCs operational at temperatures up to 200 degrees C

Li, Qingfeng; He, Ronghuan; Gao, Ji-An; Jensen, Jens Oluf; Bjerrum, Niels J.

Published in:
Electrochemical Society. Journal

Link to article, DOI:
10.1149/1.1619984

Publication date:
2003

Document Version
Publisher's PDF, also known as Version of record

Journal of The Electrochemical Society, **150** (12) A1599-A1605 (2003)
0013-4651/2003/150(12)/A1599/7/$7.00 © The Electrochemical Society, Inc.

The CO Poisoning Effect in PEMFCs Operational at Temperatures up to 200°C

Qingfeng Li,*,z Ronghuan He, Ji-An Gao, Jens Oluf Jensen, and Niels. J. Bjerrum*

Materials Science Group, Department of Chemistry, Technical University of Denmark, DK-2800 Lyngby, Denmark

The CO poisoning effect on carbon-supported platinum catalysts (at a loading of 0.5 mg Pt/cm^2 per electrode) in polymer electrolyte membrane fuel cells (PEMFCs) has been investigated in a temperature range from 125 to 200°C with the phosphoric acid-doped polybenzimidazole membranes as electrolyte. The effect is very temperature-dependent and can be sufficiently suppressed at elevated temperature. By defining the CO tolerance as a voltage loss less than 10 mV, it is evaluated that 3% CO in hydrogen can be tolerated at current densities up to 0.8 A/cm^2 at 200°C, while at 125°C 0.1% CO in hydrogen can be tolerated at current densities lower than 0.3 A/cm^2. For comparison, the tolerance is only 0.0025% CO (25 ppm) at 80°C at current densities up to 0.2 A/cm^2. The relative anode activity for hydrogen oxidation was calculated as a function of the CO concentration and temperature. The effect of CO_2 in hydrogen was also studied. At 175°C, 25% CO_2 in the fuel stream showed only the dilution effect.
 [DOI: 10.1149/1.1619984]

Manuscript submitted January 17, 2003; revised manuscript May 23, 2003. Available electronically November 12, 2003.

Polymer electrolyte membrane fuel cells (PEMFCs) generally perform best on pure hydrogen, but for many applications, especially mobile, pure hydrogen is not yet a viable option due to lack of availability and impractical storage techniques. Meanwhile, on-site generation of hydrogen by steam reforming of various organic fuels (methanol, natural gas, gasoline, etc.) is an obvious choice. The reformate gases contain, besides hydrogen and carbon dioxide, a small amount of carbon monoxide (CO). Conventional PEMFCs operate around 80°C. At this temperature a CO content as low as 10-20 ppm in the fuel feed results in a significant loss in cell performance due to CO poisoning of the electrode catalyst.[1] Therefore a strict purification of the reformate gas is necessary in order to remove CO down to a 10 ppm level. This is carried out by means of the water-gas shift reaction, preferential oxidation, membrane separation, or methanation. The main challenge for a PEMFC system, especially as a small dynamic power source for vehicles, is the complexity of the fuel processing system. Such a system currently covers 40-50% of the total system cost and considerably increases the system size, volume, weight, and time for start-up and transient response. A CO-tolerant PEMFC technology would decisively simplify the fuel cell system.

Oxidation of hydrogen on the anodic platinum catalyst is known to take place in two steps, *i.e.*, dissociative chemisorption and electrochemical oxidation. The dissociative chemisorption of a hydrogen molecule requires two free adjacent sites of the platinum surface atoms

$$\begin{array}{c} \text{H H} \\ \text{| |} \\ \text{H}_2 + \text{PtPt} \leftrightarrow \text{PtPt} \end{array} \qquad [1]$$

The electrochemical oxidation of the chemically absorbed hydrogen atoms produces two free platinum sites, two hydrogen ions, and two electrons

$$\begin{array}{l} \text{H H} \\ \text{| |} \\ \text{PtPt} \leftrightarrow \text{PtPt} + 2\text{H}^+ + 2\mathbf{e}^- \end{array} \qquad [2]$$

In case of the pure hydrogen oxidation, both step 1 and step 2 are very fast, corresponding to a very large exchange current density.[2] In a PEMFC, the hydrogen anode exhibits an overpotential of less than 100 mV under operational conditions.

When the hydrogen gas stream contains carbon monoxide (CO), CO competes with hydrogen for the adsorption sites of platinum

$$\begin{array}{c} \text{O} \\ \text{|||} \\ \text{C} \\ \text{|} \\ \text{CO} + \text{Pt} \leftrightarrow \text{Pt} \quad \text{(linearly bonded)} \end{array} \qquad [3a]$$

$$\begin{array}{c} \text{O} \\ \text{||} \\ \text{C} \\ \wedge \\ \text{CO} + \text{PtPt} \leftrightarrow \text{PtPt} \quad \text{(bridge-bonded)} \end{array} \qquad [3b]$$

Two types of bonding modes of the adsorbed CO molecules have been suggested, as shown in Reaction 3. The linearly absorbed carbon monoxide species involves one adsorption site per CO molecule, while the bridge-bonded CO species requires two adjacent platinum surface sites.[3,4] The sorption equilibrium is strongly in favor of adsorption and desorption takes place most easily via oxidation of CO to CO_2. The oxygen atoms necessary for the reaction are then obtained from the dissociation of the humidification water or the water present in the proton exchange membranes

$$\begin{array}{c} \text{H} \\ \text{|} \\ \text{O} \\ \text{|} \\ \text{Pt} + \text{H}_2\text{O} \leftrightarrow \text{Pt} + \text{H}^+ + \text{e}^- \end{array} \qquad [4]$$

in order to oxidize the adsorbed CO to CO_2 electrochemically

$$\begin{array}{l} \text{O} \quad \text{H} \\ \text{||} \quad \text{|} \\ \text{C} \quad \text{O} \\ \text{|} \quad \text{|} \\ \text{Pt} + \text{Pt} \leftrightarrow \text{PtPt} + \text{CO}_2 + \text{H}^+ + \text{e}^- \end{array} \qquad [5a]$$

* Electrochemical Society Active Member.
z E-mail: lqf@kemi.dtu.dk

$$\begin{array}{l} O\quad H \\ \|\quad | \\ C\quad O \\ \wedge\quad | \\ PtPt + PtP \leftrightarrow PtPtPt + CO_2 + H^+ + e^- \end{array} \qquad [5b]$$

The rate-determining step for sequence 4–5 is formation of the oxygen-containing adsorbate, Reaction 4. Based on these chemical and electrochemical surface processes a kinetic model has been developed.[5] At low current densities or low anodic overpotentials, the anodic oxidation of hydrogen is essentially determined by the maximum rate of hydrogen dissociative chemisorption on a small fraction of the catalyst surface area free of CO. This limiting current density is a function of the CO content in hydrogen and the operational temperature. When this limiting current density is exceeded, a much larger increase of the anode overpotential is observed due to the limited number of CO-free Pt surface sites. The electrooxidation of the adsorbed CO occurs at the potential where the oxygen-containing species are formed at the platinum surface, *i.e.*, corresponding to an anode potential around 0.5 V *vs.* RHE. Under operational conditions for a PEMFC, where the anode operates in a potential region between 0 and 0.1 V *vs.* RHE, CO is hence an inert adsorbate on the platinum catalyst surface.

Considerable efforts have been made to develop CO-tolerant electrocatalysts. Niedrach *et al.* seem to be the first, who found that addition of Ru, Rh, and Ir into Pt could improve the CO-tolerance.[6,7] Thereafter various alloys were investigated such as Pt-Sn,[8-10] Pt-Mo,[11-13] Pt(Ru)-WO_3,[14,15] and others.[16] Apparently Pt-Ru alloys are among the most promising candidates and have attracted more attention recently.[17-20] It is proposed that the presence of Ru atoms in the alloys leads to a promoter effect for the oxidation of CO adsorbates according to a bifunctional mechanism, *i.e.*, through the promotion of water dissociation and then CO oxidation. The potential for water dissociation and adsorption on Ru is lower than that on Pt (Reaction 4).[21]

Alternative approaches such as air-bleeding[22] to the CO-containing anode feed stream or addition of hydrogen peroxide[23,24] into an anode humidifier have been suggested. Even though the selectivity of the bleed oxygen is poor, *i.e.*, the bleed oxygen reacts chemically with CO and consumes hydrogen as well, it has been shown that the voltaic improvements are much greater than the coulombic losses due to the hydrogen consumption. The mechanism of the H_2O_2 addition was originally suggested as the vapor transport of the H_2O_2 from the anode humidifier to the anode where the oxygen atoms were formed by dissociative chemisorption on the anode catalysts.[23,24] However, Bellows *et al.*[25] have demonstrated that H_2O_2 decomposes at the metallic surface of the anode humidifier and the real mechanism is also by the oxygen bleed effect.

It is well known that the adsorption of CO on platinum exhibits a high negative value for the standard entropy, indicating that the adsorption is strongly favored at low temperatures.[26-28] At 130°C, for example, platinum-based catalysts can tolerate up to 1000 ppm CO, compared to only 10 ppm at 80°C.[29] Recently temperature-resistant polymer membranes, *e.g.*, the acid-doped polybenzimidazole (PBI) membranes have been developed for operation at temperatures up to 200°C.[30,31] As rationalized by Wainright *et al.*[30] and demonstrated by Savadogo *et al.*[32] and our group,[31] the high operational temperature makes it possible to improve the CO tolerance of PEMFCs. The present work examines the CO poisoning effect on the PEMFC performance based on the acid-doped PBI electrolytes at temperatures up to 200°C.

Experimental

The used PBI was synthesized from the polymerization of 3,3′-diaminobenzidine tetrahydrochloride (Aldrich) and isophthalic acid (Aldrich) in polyphosphoric acid at 170-200°C.[33] The PBI powder obtained was then dissolved in *N*,*N*-dimethylacetamide (DMAc) at 150°C under stirring. Membranes were cast using Petri dishes. The major part of the solvent was evaporated in a ventilated oven in a temperature range from 60 to 120°C. The membranes were then washed with distilled water at 80°C in order to remove the stabilizer and solvent. Traces of the solvent, DMAc, were removed by drying at 190°C. The acid-doping was carried out by immersing the membranes in phosphoric acid at room temperature for at least 1 week. The membrane of thickness about 65 μm was doped with 5.3 mol H_3PO_4 per repeating unit of PBI.

Both anodes and cathodes were prepared from carbon-supported platinum catalysts. The catalysts (20 wt% Pt) supported on carbon black (Vulcan XC-72R, Cabot) were prepared by chemical reduction of chloroplatinic acid (H_2PtCl_6). As the gas diffusion support, carbon paper (Toray TGP-H-120) was first wet-proofed by using 15% poly(tetrafluoroethylene) (PTFE) dispersion. Onto the wet-proofed carbon paper was a thin layer of PTFE-bonded (40% PTFE) carbon powder applied as the supporting layer. A slurry of Pt/C powder in 5% PBI solution in DMAc was then cast on top of the supporting layer and then dried at 190°C for a few hours. The loading of the noble metal was around 0.5 mg/cm^2. The loading of the polymer in the catalyst layer was controlled in a range from 0.6 to 0.8 mg/cm^2. The electrodes were then doped with 10% phosphoric acid. Assemblies from the acid-doped electrodes and polymer membranes were made by hot-pressing at 150°C for 10 min.

A single test cell (10 cm^2) was made of graphite plates with gas channels. Two aluminum end plates with attached heaters were used to clamp the graphite plates. Fuel and oxidant gases were supplied via mass flow controllers. Mixed gases were prepared in-line by mixing the individual gases using Bronkhorst (HI-TEC E-5514) controllers. Anode and cathode gasses were in all cases supplied under atmospheric pressure (plus the minor pressure drop in the cell). The gas flow rate was 27 cm^3/min per cm^2 of electrode working area, for both hydrogen (or its mixtures) and oxygen. The studied CO contents at different temperatures were from 0.1 to 16 vol % in the temperature range 125-200°C. Chronoamperometry for the CO poisoning and recovering was recorded at a cell voltage of 0.5 V with a recording time interval of 0.01 s. Chronoamperometric measurements showed that a steady state of the CO poisoning after the gas switch from pure hydrogen to hydrogen containing CO was reached after, *e.g.*, about 30 min at 200°C but more than 2 h at 125°C. Polarization curves were obtained by a current step potentiometry after a steady state of the poisoning was reached. Each polarization curve was measured beginning with the highest currents. Each current step lasted for 2 min.

Results and Discussion

Temperature dependence on fuel cell performance.—Figure 1 shows the current density-voltage curves for a PBI-based cell at temperatures of 125, 150, 175, and 200°C, respectively. The cell voltage can be expressed as

$$E = E_{i=0} - iR - b \log i \qquad [6]$$

where $E_{i=0}$ is the open-circuit potential (OCP), iR is the ohmic loss, and the logarithic term is the kinetic polarization of both electrodes. For high current densities an additional term describing the effect of mass-transport limitations should be included. A regression analysis of the polarization curves at different temperatures based on Eq. 6 showed a specific ohmic resistivity of the system from 0.34 to 0.26 Ω cm^2 in the temperature range from 125 to 200°C. This corresponds to a proton conductivity of 0.019 to 0.025 S/cm if the other ohmic contributions are ignored. When ohmic contributions due to electrodes, current collectors, and connections are taken into account, the obtained conductivity values could be slightly higher.

According to previous conductivity measurements[34] the membranes with similar doping levels exhibit a conductivity of about 0.02 and 0.04 S/cm at 125 and 200°C, respectively. For these conductivity measurements, the atmosphere was saturated with water vapor at room temperature before heated to the respective measuring temperatures. In the present work, water is formed through the cell

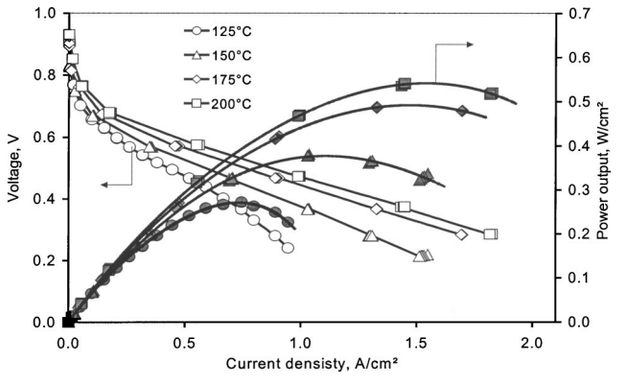

Figure 1. Polarization curves of a PBI-based PEMFCs at different temperatures. The working area of the electrodes was 10 cm^2. The PBI membrane was doped with 5.3 mol H_3PO_4 per repeat unit of the polymer. Oxygen and hydrogen were under atmospheric pressure. Hydrogen flow rate 27 mL min^{-1} cm^{-2}. Both anode and cathode were made of carbon-supported platinum catalysts (20% Pt/C) with a platinum loading of 0.5 mg Pt/cm^2. These parameters apply also to the following figures.

reaction and the humidity and therefore the conductivity could be slightly higher. These conductivity values appear to be in good agreement with the present result. These values are relatively low compared with that for Nafion membranes, which is around 0.1 S/cm at 80°C. The thickness of the used membrane is, however, relatively small, about 65 μm.

The calculated power output as a function of current density is also shown in Fig. 1. At 200°C and atmospheric pressure, a power output of around 0.42 W cm^{-2} is obtained at the cell voltage of 0.5 V. At 125°C, however, this power output is only 0.19 W/cm^2 at the cell voltage of 0.5 A/cm^2.

CO poisoning effect on the fuel cell performance.—Fuel cell performance curves with pure hydrogen and hydrogen containing carbon monoxide are shown in Fig. 2-5 at temperatures of 125, 150, 175, and 200°C, respectively. At 125°C, CO contents of 0.1, 0.5, and 1.0 vol % were tested. The CO contents of 0.5–1.0% result in significant performance losses already in the low-current-density range, while 0.1% CO shows only deviation from the pure hydrogen polarization curve at cell voltages, say, below 0.5 V.

At 150°C (see Fig. 3) under the cell voltage of 0.5 V, the current density decreases from 0.58 A/cm^2 for hydrogen to 0.52 A/cm^2 (*i.e.*, decreased by 10%) for hydrogen containing 1% CO, to 0.44 A/cm^2 (decreased by 24%) for 3% CO, to 0.37 A/cm^2 (decreased by 36%) for 5% CO, and to 0.29 A/cm^2 (decreased by 50%) for 10% CO, respectively.

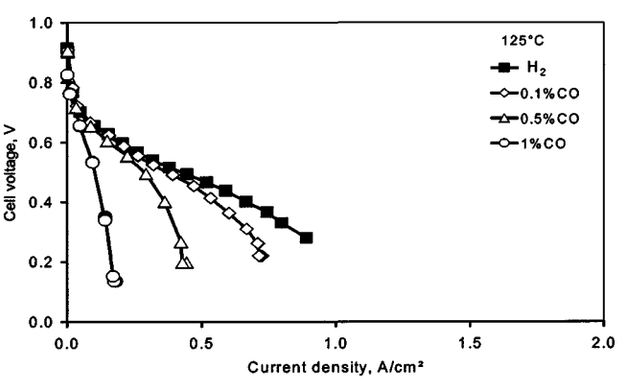

Figure 2. Polarization curves of a PBI-based PEMFC with pure hydrogen and hydrogen containing CO at 125°C. The CO concentrations are indicated in the figure.

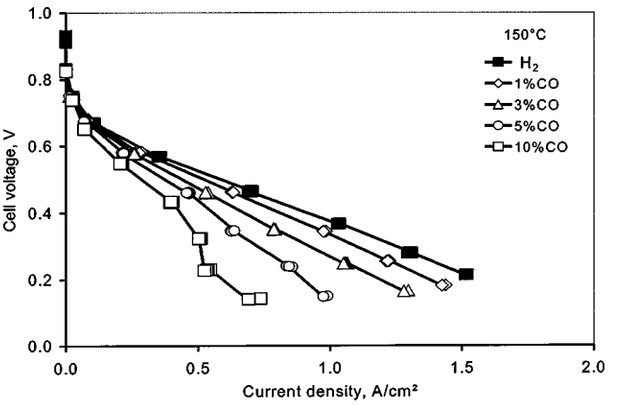

Figure 3. Polarization curves of a PBI-based PEMFC with pure hydrogen and hydrogen containing CO at 150°C. The CO concentrations are indicated in the figure.

At 175°C (see Fig. 4), however, 1% CO in hydrogen results in a decrease of 1.3% in current density at the cell voltage of 0.5 V, 5% CO of 11%, 10% CO of 19%, and 13% CO of 37%, respectively. At 200°C (Fig. 5), 3% CO in hydrogen results in no significant performance loss at current densities up to 1.0 A/cm^2 or cell voltage above 0.5 V at 200°C. Significant performance losses were observed at CO contents of 10–16% at cell voltages below 0.7 V.

At high CO contents, for example, 16% CO at 200°C, 13% CO at 175°C, and 10% CO at 150°C, a Z form of polarization curves was observed, similar to those at 80°C with CO contents higher than 100 ppm.[10,17,22] As proposed by Bellows *et al.*,[25] these three regions of the polarization curves can be interpreted using a combination of hydrogen activation (Reaction 1 and 2), adsorbed CO coverage (Reaction 3), and CO oxidation (Reaction 5). At low current densities, there are enough CO-free Pt sites to support H_2 electro-oxidation with no significant CO poisoning effect. As current density increases, the hydrogen oxidation is limited by the available Pt sites due to the CO adsorption. As a result, polarization curves exhibit a Tafel slope much higher than that for the activation hydrogen oxidation. At even higher current densities, the anode potential is high enough to promote a simultaneous oxidation of the adsorbed CO and an almost constant CO poisoning overpotential is observed.

Voltage loss due to the CO poisoning.—The CO poisoning effect can be better estimated by plotting the power output as a function of the current density. This is shown in Fig. 6, where for the purpose of clarity only a few measurements are presented.

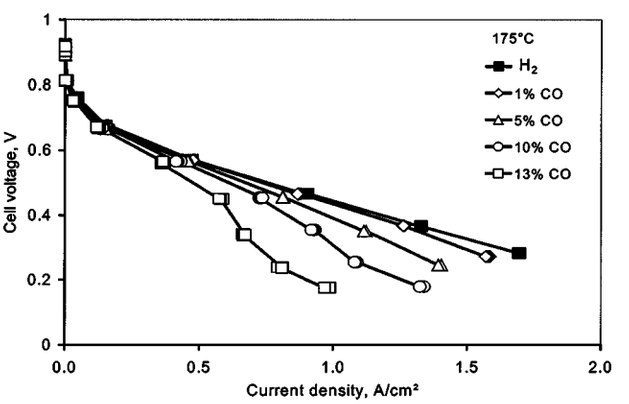

Figure 4. Polarization curves of a PBI-based PEMFC with pure hydrogen and hydrogen containing CO at 175°C. The CO concentrations are indicated in the figure.

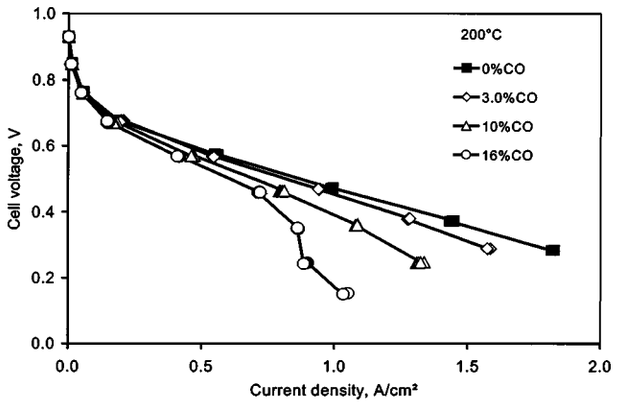

Figure 5. Polarization curves of a PBI-based PEMFC with pure hydrogen and hydrogen containing CO at 200°C. The CO concentrations are indicated in the figure.

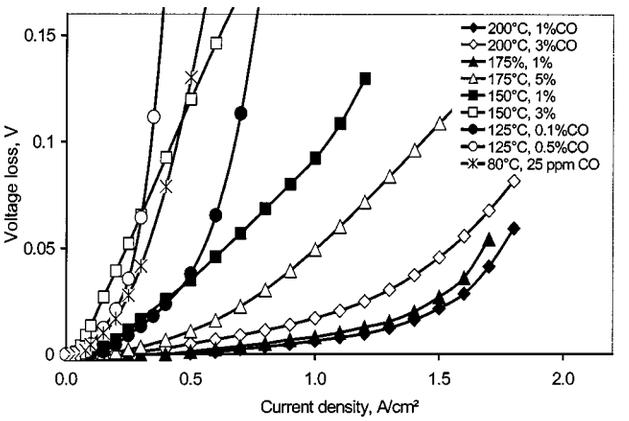

Figure 7. Voltage loss as a function of current density at different temperatures and different CO concentrations. Data for 25 ppm CO at 80°C were taken from Ref. 17.

Another way to compare the CO poisoning is to plot the cell voltage loss, *i.e.*, the voltage of CO-free hydrogen minus voltage of CO-containing hydrogen, as a function of current density. As shown in Fig. 7, the cell voltage loss is apparently a function of the CO content, anode catalyst, temperature, and current density.

By defining the CO tolerance, arbitrarily, however, as less than 10 mV, 1% CO and 3% CO in hydrogen can be tolerated at 200°C at current densities up to 1.3 and 0.8 A/cm^2, respectively. At 175 and 150°C, the tolerance of 1.0% CO was maintained at current densities up to 1.2 and 0.3 A/cm^2, respectively. At 125°C, 0.1% CO in hydrogen can only be tolerated at current densities lower than 0.3 A/cm^2. As a comparison, data for 0.0025% CO (25 ppm) in hydrogen at 80°C were taken from Ref. 17, where the CO can be tolerated at current densities up to 0.2 A/cm^2.

For an approximate estimation, as seen from Fig. 7, the voltage loss of 0.0025% CO at 80°C is located between the lines for 0.1 and 0.5% CO at 125°C or between the lines for 1 and 3% CO at 150°C, while the poisoning effects of 3% CO at 175 and 200°C are much smaller.

The relative activity of anode catalysts for hydrogen oxidation.—To characterize the CO poisoning effect, the surface coverage of platinum catalysts by CO (θ_{CO}) has been determined by a number of workers, as summarized by Wilkinson *et al.*[1] Under equilibrium conditions, the obtained θ_{CO} values varied in a wide range from 9% for 1% CO in 100% H_3PO_4 at 190°C to nearly 100% for 10–100 ppm CO in 1 M $HClO_4$ at room temperature.

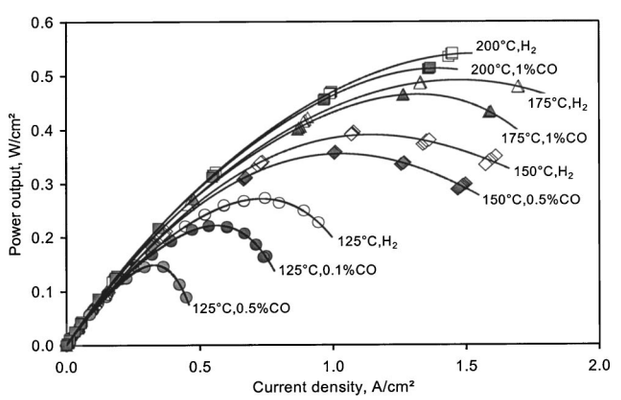

Figure 6. Power output of a PBI-based PEMFC with pure hydrogen and hydrogen containing CO. Temperatures and CO contents are indicated in the figure.

Electrochemical stripping voltammetry and polarization measurements are the two main methods for estimation of the CO surface coverage. Kinetically the measured current of the hydrogen oxidation in either presence or absence of carbon monoxide is directly related to the fraction of unblocked sites, *i.e.*, sites either occupied by H or available to hydrogen adsorption, $\theta_{unblocked}$. When the CO coverage was calculated from the measured current, it was assumed that θ_{CO} and $\theta_{unblocked}$ are simply additive, *i.e.*, $\theta_{CO}+\theta_{unblocked} = 1$. This is, however, not quite true because of the presence of other possible adsorbed species on the platinum surface.

As seen from Reaction 4, the adsorption of the dissociated water (-OH) occurs. Second, there will always be a number of uncovered surface sites, which are changing according to the adsorption equilibrium. Third, the possible mechanism (Reaction 3) of the CO adsorption by attacking the free platinum surface sites may not involve the reduction of the hydrogen coverage. Fourth, in the case of acid-doped PBI membranes, the adsorption of the acidic anion ($H_2PO_4^-$) is significant, which is well known from the research with phosphoric acid as electrolyte.[35] As reported, the adsorption of $H_2PO_4^-$ may account for up to 4% of the surface coverage in dilute phosphoric acid at room temperature for an adsorption potential of 0.1 V (*vs.* RHE). This value would be appreciably high at higher concentrations of phosphoric acid, because the mole ratio of acid to water would be shifted to a large excess of $H_2PO_4^-$ anions.

In other words, the additivity of the surface coverage of these adsorbed species should include at least the following terms

$$\theta_{CO} + \theta_{H_2} + \theta_{H_2O} + \theta_{H_2PO_4^-} + \theta_{unblocked} = 1 \qquad [7]$$

where θ denotes the fraction of surface sites covered by the species indicated, while $\theta_{unblocked}$ is the fraction of the free surface sites available for any of these absorbate species. The active surface sites available for the hydrogen oxidation, as seen from the previous expression, should include the unblocked sites ($\theta_{unblocked}$) and sites already occupied by hydrogen (θ_{H_2}).

Vogel *et al.*[26] derived the following expression for calculation of the θ_{CO} from the measured anodic currents

$$i_{(CO+H_2)}/i_{H_2} = (1 - \theta_{CO})^2 \qquad [8]$$

where i_{H_2} and i_{CO+H_2} are the anodic currents due to oxidation of hydrogen and a hydrogen-carbon monoxide mixture, respectively, at a certain overpotential. This equation implies that only adjacent free Pt sites are active for the hydrogen oxidation. It seems that this equation was justified for both planar electrodes and gas diffusion electrodes in the phosphoric acid electrolyte as the observed current-

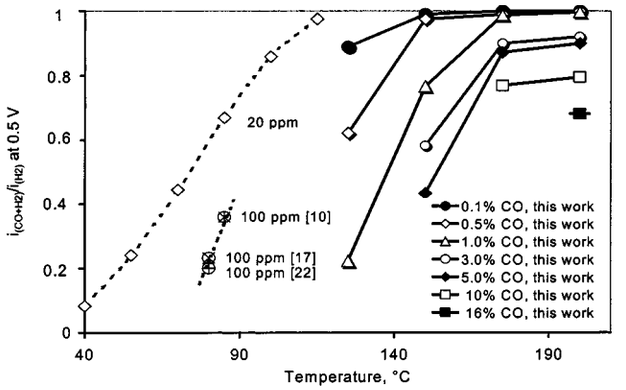

Figure 8. The calculated relative activity of the catalyst for hydrogen oxidation as a function of temperature at different CO concentrations.

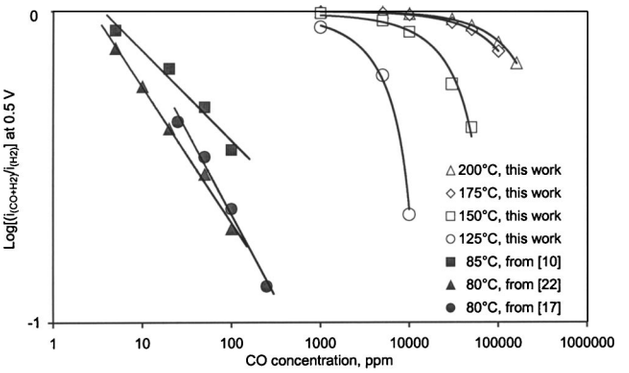

Figure 9. Logarithm of the calculated relative activity *vs.* logarithm of the CO concentration at different temperatures.

potential curves were linear and the ratio of i_{CO+H_2}/i_{H_2} did not change at low polarization. Under conditions more appropriate to the operation of PEMFCs, however, Thompsett and Cooper[36] and Igarashi *et al.*[4] suggested that the current ratio is directly proportional to $(1 - \theta_{CO})$

$$i_{(CO+H_2)}/i_{H_2} = 1 - \theta_{CO} \quad [9]$$

The measured current ratio $[i_{(CO+H_2)}/i_{H_2}]$ indicates the decrease in the hydrogen electro-oxidation activity. As Thompsett and Cooper[36] proposed, the most appropriate measure for the CO poisoning should be the decrease in fraction of active catalyst surface sites available for the hydrogen oxidation under equilibrium conditions. This measure can be further defined as the ratio of the active surface site number for the H_2 oxidation in the presence of CO to the total surface site number available for the H_2 oxidation in the absence of CO, *i.e.*, the simple ratio of poisoned H_2 oxidation current to the pure H_2 oxidation current, i_{CO+H_2}/i_{H_2}. The physical meaning of this current ratio is the relative activity of the catalysts for hydrogen oxidation at the presence of CO. A value of unity of the ratio i_{CO+H_2}/i_{H_2} indicates no change in the number of active catalyst surface sites for the hydrogen oxidation even at the presence of CO.

In the present work, a cell voltage of 0.5 V is chosen for the calculation of i_{CO+H_2}/i_{H_2} from the polarization curves with pure hydrogen and hydrogen containing CO. Figure 8 shows the calculated i_{CO+H_2}/i_{H_2} ratio as a function of temperature at different concentrations of CO. As a comparison, data for 20 ppm CO in the temperature from 40 to 115°C from Ref. 10 and for 100 ppm at 80°C from Ref. 17 and 22 and 85°C from Ref. 10 are also included.

The current ratios should have been obtained at the same anode potential. In the present work, however, they were obtained at the same cell voltage, *i.e.*, when the current density decreased as a result of CO poisoning, the cathode and ohmic potentials decreased as well. The discussion is therefore only qualitative.

These data are replotted as a function of the CO concentration (C_{CO}) at different temperatures, as shown in Fig. 9. It is seen that the dependence of the i_{CO+H_2}/i_{H_2} ratio on the CO concentration obviously is different in the temperature range below 100 and above 120°C. At 80 and 85°C for the data from Ref. 10, 17, and 22, the $\log(i_{CO+H_2}/i_{H_2})$ *vs.* $\log(C_{CO}$, in ppm) is linear with a slope from -0.3 to -0.55, *i.e.*, the logarithm of i_{CO+H_2}/i_{H_2} ratio is approximately proportional to the logarithm of $(C_{CO})^{-1/3--1/2}$. In the temperature range from 125 to 200°C, however, the i_{CO+H_2}/i_{H_2} ratio is a linear function of the C_{CO} with a slope of -0.0003 at 200°C, -0.0002 at 175°C, -0.0012 at 150°C, and -0.0077 at 125°C, respectively. The decrease of the slope with increasing temperature apparently indicates the temperature dependence of the CO poisoning effect.

The CO_2 poisoning effect.—Reformed hydrogen is always mixed with a significant amount of carbon dioxide, CO_2, due to the carbon atoms of the primary fuel. It is known that the presence of CO_2 in the fuel stream does have influence on the PEMFC performance at low temperatures,[1,37] though the poisoning effect is limited compared to that of CO. While CO_2 itself is considered as inert, the poisoning effect is attributable to the formation of CO by the reverse water-gas shift reaction

$$H_2 + CO_2 = H_2O + CO \quad [10]$$

Under operational conditions of the Nafion-based PEMFCs, *i.e.*, the well-humidified fuel feed and low temperatures (*ca.* 80°C), the formed CO in a typical gas mixture of 75% H_2 and 25% CO_2 could be in the range 20-50 ppm. The formation of CO is apparently dependent on temperature and the water content in the fuel feed. At 100°C with a water content of 15%, for example, it was calculated that the amount of CO in the gas mixture would increase up to *ca.* 250 ppm.[37] This presents a significant poisoning effect on the PEMFC performance at 80°C. The effect may be even more pronounced because the adsorption shifts the equilibrium further toward formation of CO. This poisoning effect was found to be less when Pt-Ru alloy catalysts were used as the anode than the pure platinum catalyst.[1]

With PBI-based polymer membrane electrolytes, the fuel cell operates without humidification of reactant gases. The absence of water in the anode feed gas shifts the equilibrium of Reaction 10. As Baschuk and Li calculated,[38] as high as 6500 ppm CO can be formed at zero humidity and 100°C. By extrapolating these data of Ref. 37 and 38 it seems that CO formation in the studied temperature range from 125 to 200°C would be in a range up to 1%, which is within the tolerance limit.

Figure 10 shows polarization curves obtained at 175°C with pure hydrogen and hydrogen containing 25% CO_2. A small performance loss is observed especially at higher current densities. The total gas flow rate for both pure hydrogen and the hydrogen-CO_2 mixture was kept constant, about 27 mL min^{-1} cm^{-2}, corresponding to a maximum theoretical current density of 3.8 A/cm^2 for pure hydrogen and 2.9 A/cm^2 for hydrogen containing 25% CO_2. When the total gas flow rate remains unchanged, the replacement of the 25% CO_2 in hydrogen by nitrogen gives the same performance loss, attributable to a mere dilution effect or, more exact, a lowering of the hydrogen partial pressure (see Fig. 10).

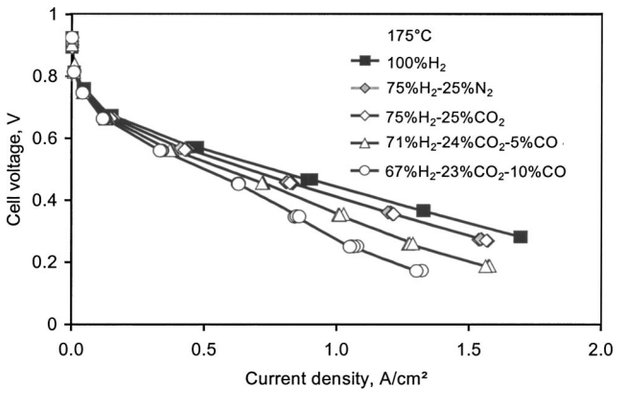

Figure 10. Polarization curves of a PBI-based PEMFC with pure hydrogen and hydrogen containing CO_2 and CO at 175°C. The total flow rate of hydrogen and mixed gases was 27 mL min^{-1} cm^{-2}.

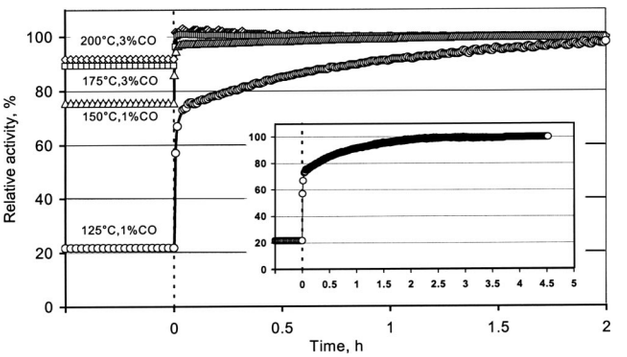

Figure 12. The relative activity of the platinum catalyst as a function of time during the recovery after the CO poisoning. Time = 0 was the moment when the fuel gas was switched from a H_2-CO mixture to pure hydrogen. The cell voltage was held at 0.5 V. The inserted figure is a zoom out of the curve for 125°C.

Addition of CO into the 75% H_2 and 25% CO_2 mixture results in a further decrease in performance, as shown in Fig. 10. Comparison of Fig. 10 and 4 shows no significant change in the CO poisoning effect when 25% CO_2 is introduced at 175°C.

The current decay as a function of time.—The CO poisoning effect is a slow process. Oetjen *et al.*[17] reported that a steady-state polarization curve at 80°C with 100 ppm CO was only obtained after 210 min. The current density was 250 mA/cm^2 between the scans. The process was found to be dependent on the CO concentration and the catalysts. For a PtRu catalyst a steady-state voltage at 400–500 mA/cm^2 was attained after about 100 min.[17,24] A transient study of the CO poisoning effect by Bauman *et al.*[39] showed that the performance loss upon a switch from 0 to 100 ppm CO at 80°C was completed in several minutes. These time frames are apparently dependent on the gas flow rate, setup construction, electrode diffusion layer, catalyst type and loading, CO coverage and adsorption type, temperature, and other parameters.

In Fig. 11 the activity of the applied Pt catalyst is plotted as a function of time at selected temperatures and CO levels. It is seen that the poisoning rate highly depends on temperature. At 125°C, a steady-state current density at a cell voltage of 0.5 V was nearly reached about 1.3 h after switching the fuel gas from pure hydrogen to 1% CO mixture. At 150 and 175°C, the time was found to be about 50 min for 1% CO and 10 min for 3% CO, respectively. At 200°C, however, the cell performance went to a minimum immediately as the CO-containing fuel was applied and reached a steady-state current density after about half an hour.

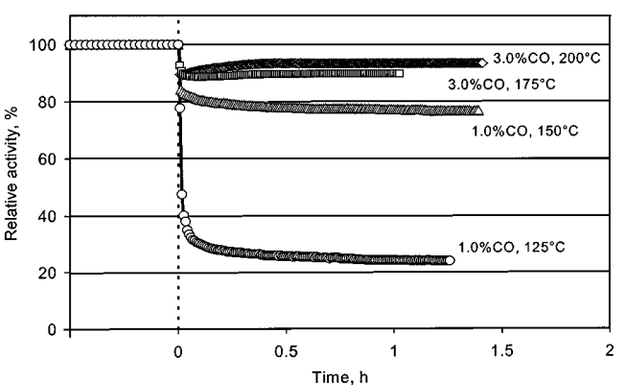

Figure 11. The relative activity of the platinum catalyst as a function of time during the onset of the CO poisoning at different temperatures. Time = 0 was the moment when the fuel gas was switched from pure hydrogen to a H_2-CO mixture. The cell voltage was held at 0.5 V.

It is known that CO adsorption on a platinum surface is reversible. Figure 12 shows that the cell performance can be restored after poisoning. After a steady-state poisoning was reached, the fuel gas was switched back from the H_2-CO mixture to pure hydrogen while the cell voltage was maintained at 0.5 V. It is seen from the figure that the previous performance for pure hydrogen can be restored almost immediately from 3% CO at 200 and 175°C. At 150°C it took about 1 h to restore the performance from 1% CO. At 125°C, however, the recovery of the poisoning effect is very slow; more than 3 h were necessary. It seems that the process to restore the initial cell performance after the CO poisoning is much slower than the poisoning effect, especially at low temperatures, though Divisek *et al.*[24] reported the contrary results.

One possible explanation could be that the water content near the anode affects the rate of recovery. This is most likely if the recovery proceeds via water adsorption (see Eq. 4 and 5). Humidified hydrogen, which always is used for Nafion-based cells, is a good water source. In the present work nonhumidified hydrogen was applied and consequently water was only supplied through the back-diffusion via the membrane. The water content is thus expected to be much lower, resulting in a lower rate of CO oxidation.

Conclusions

With the acid-doped PBI membranes as electrolyte, the effect of CO poisoning on carbon-supported platinum catalysts in PEMFCs has been investigated in a temperature range from 125 to 200°C. By defining the CO tolerance as a cell voltage loss less than 10 mV, the CO poisoning effect is evaluated. It was found that 1 and 3% CO in hydrogen can be tolerated at 200°C at current densities up to 1.3 and 0.8 A/cm^2, respectively. At 175 and 150°C, the tolerance to 1.0% CO can be maintained at current densities up to 1.2 and 0.3 A/cm^2, respectively. At 125°C, however, 0.1% CO in hydrogen can only be tolerated at current densities lower than 0.3 A/cm^2. This should be compared with a tolerance to 0.0025% CO (25 ppm) at 80°C at current densities up to 0.2 A/cm^2. The relative activity of the catalyst for hydrogen oxidation in the presence of CO was calculated from the measured polarization currents at 0.5 V as a function of the CO concentration and temperature. Only a dilution effect was observed for CO_2 at a level up to 25% at 175°C. The onset and the recovery of the CO poisoning are strongly dependent on temperature.

Acknowledgment

This work has received financial support from the European Commission in the 5th Framework Program (contract no. ENK5-CT-2000-00323).

The Technical University of Denmark assisted in meeting the publication costs of this article.

References

1. D. P. Wilkinson and D. Thompsett, in *Proceedings of the Second International Symposium on New Materials for Fuel-Cell and Modern Battery Systems*, O. Savadogo and P. R. Roberge, Editors, p. 266, Montréal, Canada (1997).
2. R. M. Q. Mello and E. A. Ticianelli, *Electrochim. Acta*, **42**, 1031 (1997).
3. M. Watanabe and S. Motoo, *J. Electroanal. Chem. Interfacial Electrochem.*, **206**, 197 (1986).
4. H. Igarashi, T. Fujino, and M. Watanabe, *J. Electroanal. Chem.*, **391**, 119 (1995).
5. T. Springer, T. Zawodzinski, and S. Gottesfeld, in *Electrode Materials and Processes for Energy Conversion and Storage IV*, J. McBreen, S. Mukerjee, and S. Srinivasan, Editors, PV 97-13, p. 15, The Electrochemical Society Proceedings Series, Pennington, NJ (1997).
6. L. W. Niedrach, D. W. McKee, J. Paynter, and I. F. Danzig, *Electrochem. Technol.*, **5**, 318 (1967).
7. D. W. McKee, L. W. Niedrach, J. Paynter, and I. F. Danzig, *Electrochem. Technol.*, **5**, 419 (1967).
8. S. Motoo and M. Watanabe, *J. Electroanal. Chem. Interfacial Electrochem.*, **69**, 429 (1976).
9. H. A. Gasteiger, N. M. Markovic, and P. N. Ross, Jr., *J. Phys. Chem.*, **99**, 8945 (1995).
10. S. J. Lee, S. Mukerjee, E. A. Ticianelli, and J. McBreen, *Electrochim. Acta*, **44**, 3283 (1999).
11. B. N. Grgur, G. Zhuang, N. M. Markovic, and P. N. Ross, Jr., *J. Phys. Chem. B*, **101**, 3910 (1997).
12. B. N. Grgur, N. M. Markovic, and P. N. Ross, Jr., *J. Phys. Chem.*, **102**, 2494 (1998).
13. S. Mukerjee, S. J. Lee, E. A. Ticianelli, J. McBreen, B. N. Grgur, N. M. Markovic, P. N. Ross, J. R. Giallombardo, and E. S. De Castro, *Electrochem. Solid-State Lett.*, **2**, 12 (1999).
14. K. Y. Chen, P. K. Shen, and A. C. C. Tseung, *J. Electrochem. Soc.*, **142**, L185 (1995).
15. K. Y. Chen, Z. Sun, and A. C. C. Tseung, *Electrochem. Solid-State Lett.*, **3**, 10 (2000).
16. G. L. Holleck, D. M. Pasquariello, and S. L. Clauson, in *Proton Conducting Membrane Fuel Cells II*, S. Gottesfeld and T. F. Fuller, Editors, PV 98-27, p. 150, The Electrochemical Society Proceedings Series, Pennington, NJ (1998).
17. H. F. Oetjen, V. M. Schmidt, U. Stimming, and F. Trila, *J. Electrochem. Soc.*, **143**, 3838 (1996).
18. M. C. Denis, G. Lalande, D. Guay, J. P. Dodelet, and R. Schulz, *J. Appl. Electrochem.*, **29**, 951 (1999).
19. S. D. Lin, T.-C. Hsiao, J.-R. Chang, and A. S. Lin, *J. Phys. Chem. B*, **103**, 97 (1999).
20. T. J. Schmidt, M. Noeske, H. A. Gasteiger, and R. J. Behm, *J. Electrochem. Soc.*, **145**, 925 (1998).
21. A. Gasteiger, N. Markovic, P. N. Ross, Jr., and E. J. Cairns, *J. Phys. Chem.*, **98**, 617 (1994).
22. S. Gottesfeld and J. Pafford, *J. Electrochem. Soc.*, **135**, 2651 (1988).
23. V. M. Schmidt, H. F. Oetjen, and J. Divisek, *J. Electrochem. Soc.*, **144**, L237 (1997).
24. J. Divisek, H.-F. Oetjen, V. M. Schmidt, and U. Stimming, *Electrochim. Acta*, **43**, 3811 (1998).
25. R. J. Bellows, E. Marucchi-Soos, and R. P. Reynolds, in *Proton Conducting Membrane Fuel Cells II*, S. Gottesfeld and T. F. Fuller, Editors, PV 98-27, p. 121, The Electrochemical Society Proceedings Series, Pennington, NJ (1998).
26. W. Vogel, J. Lundquist, P. Ross, and P. Stonehart, *Electrochim. Acta*, **20**, 79 (1975).
27. H. P. Dhar, L. G. Christner, A. K. Kush, and H. C. Maru, *J. Electrochem. Soc.*, **133**, 1574 (1986).
28. H. P. Dhar, L. G. Christner, and A. K. Kush, *J. Electrochem. Soc.*, **134**, 3021 (1987).
29. G. Xiao, Q. Li, H. A. Hjuler, and N. J. Bjerrum, *J. Electrochem. Soc.*, **142**, 2890 (1995).
30. J. S. Wainright, J.-T. Wang, D. Weng, R. F. Savinell, and M. Litt, *J. Electrochem. Soc.*, **142**, L121 (1995).
31. Q. Li, H. A. Hjuler, and N. J. Bjerrum, *J. Appl. Electrochem.*, **31**, 773 (2001).
32. O. Savadogo and B. Xing, *J. New Mater. Electrochem. Syst.*, **3**, 343 (2000).
33. Y. Iwakura, K. Uno, and Y. Imai, *J. Polym. Sci., Part A: Gen. Pap.*, **2**, 2605 (1964).
34. R. He, Q. Li, G. Xiao, and N. J. Bjerrum, *J. Membr. Sci.*, Submitted (2002).
35. G. Kohlmayr and P. Stoneheart, *Electrochim. Acta*, **18**, 211 (1973).
36. D. Thompsett and S. J. Cooper, Abstract 607, p. 948, The Electrochemical Society Meeting Abstracts, Vol. 94-2, Miami, FL, Oct 9-14, 1994.
37. F. A. de Bruijn, D. C. Papageorgopoulos, E. F. Sitters, and G. J. M. Janssen, *J. Power Sources*, **110**, 117 (2002).
38. J. J. Baschuk and X. Li, *Int. J. Energy Res.*, **25**, 695 (2001).
39. J. W. Bauman, T. A. Zawodzinski, Jr., and S. Gottesfeld, in *Proton Conducting Membrane Fuel Cells II*, S. Gottesfeld and T. F. Fuller, Editors, PV 98-27, p. 136, The Electrochemical Society Proceedings Series, Pennington, NJ (1998).